Journal of Pharmacological Biomolecules and Therapeutics

ETERNO PRESS

Article

In Vitro Study of Anticancer Activity of Biosynthesized ZnO and Co-ZnO Nanoparticles on Human Brain Glioblastoma Cells

Azadeh Samani[1], Mostafa Azizi[1,2,*]

[1]Cellular and Molecular Research Center, Birjand University of Medical Sciences, Birjand, Iran

[2]Microbiological Research Center, Birjand University of Medical Sciences, Birjand, Iran

[*]Corresponding author: Mostafa Azizi, Mostafa777azizi@gmail.com

Abstract

A successful attempt was made to utilize leaf extract of *Prosopis fracta* for the environmentally friendly and straightforward synthesis of zinc oxide (ZnO) and cobalt-doped zinc oxide (Co-ZnO) nanoparticles. This synthesis was characterized using analytical techniques including field emission scanning electron microscopy (FESEM) and powder X-ray diffraction (PXRD). The presence of finely doped cobalt within the zinc oxide structure was confirmed by PXRD and energy dispersive X-ray (EDX) data. The FESEM analysis revealed a spherical morphology for both ZnO and Co-ZnO nanoparticles. The cytotoxicity of the synthesized nanoparticles was surveyed against brain glioblastoma cells (U87) through the WST-1 assay. Compared to the results obtained from pure nanoparticles, the doped nanoparticles demonstrated a significantly greater toxicity towards U87 cells. Experimental results presented that Co-ZnO nanoparticles created a pronounced cytotoxic impact. Thus, it concluded that doping process applied to ZnO nanoparticles enhanced their inhibitory effect on U87 cells.

Keywords

Cobalt doped zinc oxide, FESEM, U87, WST-1

Article History

Received: 31 December 2025 Revised: 05 June 2026

Accepted: 08 July 2026 Available Online: 15 July 2026

1. Introduction

Over recent years, nanoscale engineering has emerged as a highly promising strategy across various therapeutic domains. Among engineered nanoscale entities, metallic nanostructures have attracted substantial attention both as stand-alone therapeutic agents and as advanced carriers designed for the targeted delivery of pharmacological compounds against complex diseases. Zinc oxide (ZnO) nanostructures, a prominent subclass of metal oxide nanomaterials, exhibit exceptional ultraviolet radiation attenuation combined with optical transparency in the visible spectrum, establishing their utility as advanced photoprotective formulations for dermatological applications [1,2]. Furthermore, studies have elucidated their antimicrobial and antineoplastic functions, mechanisms largely attributed to their ability to induce cellular redox imbalance [3]. In addition to these inherent therapeutic properties, ZnO nanostructures also serve as versatile platforms for pharmaceutical payload delivery. ZnO nanostructured variants with characteristic dimensions exceeding 100 nanometers display favorable biocompatibility profiles, reinforcing their suitability for drug carrier applications [4].

ZnO is a conventional semiconductor characterized by a wide electronic bandgap. This distinctive electronic configuration underpins its applicability across multiple biomedical interventions, including cancer suppression, microbial inhibition, and antifungal therapies [5]. The therapeutic mechanisms of ZnO nanostructures predominantly arise from their ability to catalyze ROS formation, triggering irreversible cellular damage when endogenous antioxidant defenses become overwhelmed [6]. The semiconductor physics governing ZnO directly modulates its ROS-generating potential. In semiconductor frameworks, electron energy states occupy discrete bands separated by a forbidden energy zone called the bandgap, the interval extending from the upper boundary of electron-populated bonding states to the lower threshold of the empty delocalized transport zone. In crystalline ZnO, this bandgap measures approximately 3.3 electron volts. Photonic energy within the ultraviolet range possesses sufficient quantum energy to promote the highest-energy electron-filled orbital into the unoccupied mobile charge region, thereby producing complementary mobile charge carriers of opposite polarity. These photogenerated charge carriers subsequently migrate to the nanoparticle periphery, where electrons reduce molecular oxygen while holes oxidize hydroxyl species, culminating in superoxide anion and hydroxyl radical formation [5,7].

Notably, even under ambient illumination without ultraviolet exposure, ZnO nanostructures harbor substantial populations of positive charge vacancies in the uppermost occupied energy stratum and/or mobile negative charge carriers in the accessible unoccupied transport region. This phenomenon arises from intrinsic crystallographic imperfections characteristic of nanoscale architectures. The resulting reactive oxygen species (ROS) initiate self-perpetuating redox cascades within cellular environments, culminating in permanent oxidative injury to biomolecular constituents [8]. Additional cytotoxic pathways contributing to ZnO nanostructure bioactivity include programmed cell death and unregulated cellular disintegration mechanisms [9,10]. ROS-mediated genomic lesions activate apoptotic signaling cascades [11]. This sequence leads to apoptosome assembly and the sequential activation of caspase proteases [12]; proteolytic cleavage of critical cellular substrates ultimately executes programmed cell death. An alternative dissolution-mediated mechanism has also been proposed, wherein internalized ZnO aggregates undergo rapid solubilization within acidic lysosomal compartments of phagocytic cells, releasing zinc ions that independently trigger apoptotic pathways [9].

The antineoplastic activity of ZnO nanostructures operates through dual mechanisms: ROS-mediated oxidative stress and apoptosis induction, coupled with distinctive electrostatic interactions. The surface charge characteristics of these nanostructures derive from hydroxyl moieties chemisorbed onto their exterior interfaces. In aqueous environments under alkaline conditions, surface proton dissociation yields negatively charged interfaces featuring deprotonated oxygen termini (ZnO^{-}). Conversely, under acidic conditions, proton adsorption generates positively charged surfaces ($ZnOH_2^{+}$) [5,13]. With an isoelectric point occurring between pH 9 and 10, ZnO nanostructures maintain a substantial positive surface potential under physiological pH conditions [14]. Malignant cellular membranes, in contrast, display elevated concentrations of anionic phospholipid components, particularly phosphatidylserine, on their outer leaflets, alongside pronounced negative transmembrane potentials [15,16]. This electrostatic complementarity at the interface between cationic nanoscale constructs and anionic malignant cellular boundaries enhances cellular internalization, phagocytic uptake, and consequent cytotoxic potency [17].

These multifaceted attributes position ZnO nanostructures as viable candidates for nanotherapeutic deployment or as synergistic enhancers alongside conventional chemotherapeutics. Research efforts have additionally explored the integration of pharmaceutical payloads with ZnO nanostructures to enhance cellular internalization and achieve combinatorial therapeutic outcomes. Surface engineering strategies have been implemented to improve colloidal stability and cell-type selectivity. Experimental findings demonstrated that surface functionalization using polyethylene glycol, Triton X-100 surfactant, or hyaluronic acid matrices preserved intrinsic antineoplastic efficacy while improving biocompatibility profiles toward non-malignant cell populations through protective biopolymeric coatings [18-20]. Furthermore, combinatorial investigations pairing ZnO nanostructures with established chemotherapeutic agents, including doxorubicin, cisplatin, and paclitaxel, revealed substantially enhanced cytotoxic responses compared to monotherapy regimens [8,21].

Selective cytotoxicity toward malignant cell populations has received empirical confirmation using murine myogenic precursor and preadipocyte differentiation platforms. Elevated caspase-3 enzymatic activity coupled with amplified ROS generation was observed preferentially in C2C12 cultures relative to 3T3-L1 counterparts, confirming targeted apoptotic induction in neoplastic lineages [22]. Wahab and colleagues [23] further demonstrated cellular selectivity by evaluating ZnO nanostructure toxicity across malignant T98G glioblastoma and KB epidermoid carcinoma lines versus non-transformed HEK renal epithelial cells. Results indicated maximal cytotoxicity against T98G cells, intermediate effects on KB populations, and minimal impact on normal HEK cells. Additional investigations examining size-dependent (5 nm versus 200 nm) and interfacial molecular interaction phenomena confirmed consistent preferential toxicity toward malignant cultured cell populations without compromising normal human benign counterparts across heterogeneous molecular defense networks [24,25].

Leveraging their intrinsic antineoplastic properties, ZnO nanostructures have been engineered as carriers for active pharmaceutical ingredients with the objective of potentiating chemotherapeutic efficacy. Hypotheses suggest that drug loading onto ZnO platforms may amplify therapeutic indices through synergistic mechanisms. To further refine tumor targeting precision, nanostructure surfaces have been functionalized with molecular recognition elements, including vitamin-derived targeting entities alongside engineered oligonucleotide binders formulated to selectively adhere to pterin-transport proteins and glycosylated epithelial surface antigens, both displaying elevated abundance on tumorigenic plasma membranes [26-28]. Han and colleagues integrated targeted photodynamic therapy with conventional chemotherapy using aptamer-decorated, drug-loaded ZnO nanostructures. Transcriptional upregulation of caspase-3 confirmed apoptosis execution at the gene expression level. Aptamer conjugation markedly increased intracellular nanostructure accumulation within malignant cells, suggesting that such multimodal therapeutic platforms may achieve enhanced neoplastic cytotoxicity through combined mechanistic pathways [26].

As the most prevalent and aggressive primary brain tumor, glioblastoma can arise in any part of the brain's nervous tissue [29] and confers a very short median survival time. In contrast, only approximately three percent of affected individuals demonstrate sustained viability exceeding forty-eight months [29]. This widely utilized intracranial glial malignancy culture model holds a distinguished status among human-derived grade IV astrocytoma experimental systems, although previous assessments have claimed that brain tumors surpass other types of human tumors in clinical significance. Considering the lower probability of these cancers occurrence when compared to the other kinds, such as gastrointestinal cancers, yet the crucial stance of their tumor type is indisputable due to their acute difficulties, deficiency of pertinent treatment, and supremely high metastasis [30].

The effectiveness of current treatments for glioblastoma is quite disheartening, as a significant proportion of cases experience recurrence. This is primarily due to the inability of chemical drugs to penetrate the brain across the blood-brain barrier. Such a phenomenon facilitates tumor recurrence, aided by the self-regenerative properties of glioma stem cells [29], culminating in a pronounced reduction of typical survival metrics among individuals afflicted by aggressive glial malignancies. Deleterious consequences arising from therapeutic agent co-administrations, along with the protracted treatment duration, substantial financial burden, and suboptimal clinical outcomes inherent in current intervention protocols, underscore the growing global need for developing pioneering methodologies and tactical frameworks to mitigate this pathological condition [31].

Sub-100-nanometer construct engineering embodies a rapidly evolving domain with substantial promise to advance pharmaceutical manufacturing, treatment modalities, and disease identification frameworks for heterogeneous pathological conditions, including malignant neoplasms [32,33]. Elemental cation-oxygen composite submicron entities have been the subject of sustained scholarly examination as a promising therapeutic avenue for malignant neoplasms [34,35]. The manufacture and creation of these entities may serve as highly cost-effective strategies, stemming from the abundant geological presence of inorganic ZnO mineral reserves. Notably, nanoscale ZnO composites manifest characteristics that may position them as especially potent agents against glioblastoma multiforme [35].

The fabrication of ZnO nanostructures using ecologically sustainable precursors, including naturally derived biomolecules, polymeric macromolecules [36,37], botanical foliar extracts [38-40], prokaryotic microorganisms [41], fungal species [42,43], and photosynthetic microalgae [44], offers distinct advantages in terms of environmental stewardship and physiological compatibility for pharmacological deployment, while simultaneously eliminating the use of hazardous reagents during synthetic procedures. The integration of phytogenic extracts into nanofabrication protocols has emerged as an operationally straightforward yet highly efficient alternative to conventional physicochemical techniques. Sustainable nanostructure production paradigms have attracted considerable scholarly interest due to their ecological advantages, cost-effectiveness, and expanding implementation across therapeutic nanocarrier systems, catalytic pharmaceutical synthesis, nanoscale optoelectronic devices, and related technological domains [45]. This research frontier represents an innovative and rapidly advancing scientific discipline in which continuous methodological refinement promises substantial future impact. Biologically derived and ecologically conscious ZnO nanostructure fabrication methodologies exhibit negligible cytotoxicity, biological safety, and tissue compatibility, rendering them suitable for pharmaceutical delivery platforms, dermo-cosmetic formulations, and biomedical composite reinforcement applications [46].

Botanical extract utilization represents an accessible pathway for ZnO nanostructure biosynthesis. Sangeetha et al. used foliar extracts of *Aloe barbadensis miller* to generate ZnO nanostructures by comparing chemical and biological protocols. The reaction between zinc nitrate precursors and *Aloe vera* leaf extracts produced exceptionally stable spherical nanostructures. A conversion efficiency exceeding 95% was achieved when the leaf extract concentration exceeded 25% (v/v). Microscopic characterization using scanning and transmission electron microscopy revealed polydisperse nanostructures with an average diameter of 25-40 nanometers. The nanostructures were predominantly spherical, and dimensional control could be achieved by systematically modulating the concentration of the botanical extract [47,48].

Therefore, this study focused on eco-compatible synthesis of ZnO and cobalt-integrated zinc oxide (Co-ZnO) nanoparticles using *Prosopis farcta* plant extract. Considering zinc-oxygen's established attributes and oncological treatment urgency, this investigation examined these laboratory-synthesized ultrafine constructs' influence on cellular demise within human intracranial grade IV glial malignancy cultures (U87).

2. Experimental

2.1 Extraction of *Prosopis Farcta*

Plant material from *Prosopis farcta* was first weighed, then mixed with purified water at a 1:10 (w/v) ratio. The mixture was subjected to orbital shaking at 150 rpm for 15 hours. The resulting suspension was then filtered through a porous membrane, and the filtrate was retained for subsequent analyses.

2.2 Synthesis of ZnO Nanoparticles

To synthesis of nanoparticles, 15 mL (0.1 g) of extract was added to 0.5 mol/L of solution of $Zn(NO_3)_2{\cdot}9H_2O$ (Merck). This solution stirred. Afterwards, the obtained solution dried at 60 ℃ for10 hours. The resulted raw powder was calcinated at 600 ℃ for 2.5 hours. the obtained white powder was ZnO nanoparticles.

2.3 Synthesis of Co-ZnO Nanoparticles

For nanoscale assembly production, fifteen-milliliter phytoextract portions were introduced into aqueous media containing half-molar zinc nitrate nonahydrate alongside fifty-millimolar cobalt nitrate hexahydrate (commercial origin). The admixture underwent sustained agitation for 3 hours at 70 ℃, followed by ten-hour evaporative drying. The desiccated residue subsequently received calcination at 600 ℃ for 2 hours, yielding cobalt-doped zinc-oxygen nanoscale constructs. A visual workflow schematic appears in the Figure 1.

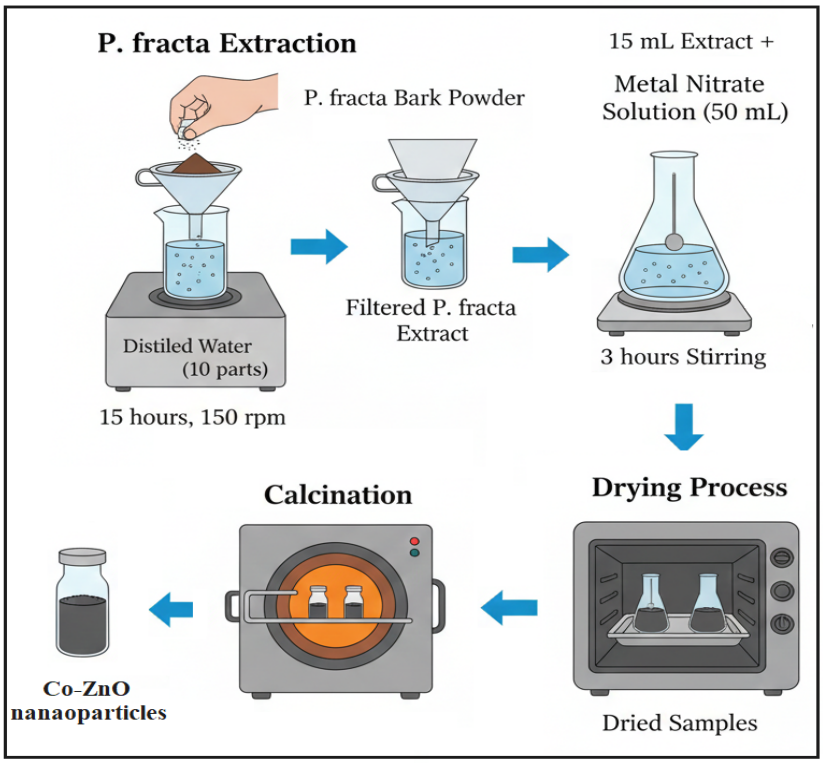

Figure 1. Schematic image of preparation of Co-ZnO nanoparticles.

2.4 Characterization of Nanoparticles

Multiple characterization protocols were implemented to define physicochemical attributes of ZnO and Co-ZnO nanoscale entities. Extended structural order within artificially generated specimens was evaluated via powder X-ray diffraction using copper characteristic radiation on PANalyticalX'Pert PRO MPD system. Lattice phonon signatures were captured through inelastic light scattering analysis activated by 532 nanometer monochromatic excitation. Furthermore, the surface morphology of the samples was examined via FESEM (MIRA3 TESCAN, Czech) analysis.

2.5 Cytotoxicity Test

2.5.1 Cell Culture

This experimental segment concentrated on measuring cell death induction by nanoscale entities directed toward human cerebral grade IV glial malignancy cultures. Toward this aim, previously acquired cryopreserved specimens from an Iranian national biomedical institution underwent defrosting before nutrient medium propagation. The cellular material was thereafter relocated into conical polymeric sedimentation containers and subjected to rotational separation at eight hundred thirty-three cycles per minute for a nine-minute duration. After decantation of the supernatant phase, nutrient-replete cultivation matrix was incorporated with the cellular sediment, and the resultant dispersions distributed into sterile culture containers. Cellular propagation employed DMEM medium augmented with ten percent bovine fetal serum derivative, one hundred micrograms per milliliter aminoglycoside antibiotic, and 100 units per milliliter penicillin-class agent to inhibit contaminant proliferation. Environmental maintenance at 37 ℃ under 5% carbon dioxide atmosphere subsequently enabled cellular multiplication and population amplification.

2.5.2 WST-1 Test

Cellular lethality induced by nanoscale entities toward U87 cells was quantified employing a tetrazolium-derived metabolic activity detection methodology, with five concentration tiers examined across a progressive spectrum from one to one thousand micrograms per milliliter; basal nutrient matrix served as the baseline reference condition. The protocol commenced with deposition of a cellular dispersion containing ten thousand units per compartment into a 96-well plate, at physiological temperature. After validation of cellular adhesion to the substrate interface, the cultivation matrix was withdrawn from discrete chambers of the 96-well plate. One hundred microliters of laboratory-prepared nanoscale entity suspension were thereafter dispensed into the compartments, followed by supplementary twenty-four-hour thermoregulated atmospheric exposure at 37 ℃ under 5% carbon dioxide conditions.

Following the initial thermal maintenance interval, ten-microliter aliquots of tetrazolium-derived redox indicator reagent were dispensed into all microtiter compartments, succeeded by four-hour supplementary environmental conditioning. Optical density values for each specimen were thereafter recorded at four hundred ninety nanometer spectral wavelength via microplate spectrophotometric instrumentation. Each sample was tested in triplicate. The subsequent analytical phase involved computation of metabolically active cellular population proportions through application of the mathematical relationship specified in Equation (Eq. 1).

$$\text{Cell viability \%} = [100 \times (\text{sample abs})/ (\text{control abs})] \quad \text{(Eq. 1)}$$

2.5.3 Fifty Percent of Cellular Proliferation Activity (IC_{50})

The conduction of the probit examination required the employment of SPSS for measuring pharmaceutical agent concentrations together with nanoscale entity dosages, which proved capable of attenuating fifty percent of cellular proliferation activity (IC_{50}). Additionally, this method was exerted to calculate the percent of controlling the cell growth towards the applied volume.

3. Results and Discussion

3.1 PXRD Outcome

Figure 2 displays scattering intensity data acquired from powder X-ray diffraction examination of ZnO and Co-ZnO nanoparticles. Examination of the undoped ZnO material revealed scattering maxima at diffraction angles ranging from 31.91° to 69.21°, indexed to lattice planes with Miller indices (100) through (201). This signature validates the formation of a hexagonal wurtzite-type crystalline architecture in the pure compound (JCPDS card no. 36-1451) [34]. The finding illustrated in Figure 2 demonstrates modest angular displacement of the ZnO (101) Bragg reflection upon cobalt incorporation; this shift likely stems from heteroatomic substitution of host cations within the crystalline framework. Coherent scattering domain dimensions were subsequently derived through diffraction peak width analysis methodology [49], yielding values of 18.65 nm for pristine ZnO and 29.8 nm for 3% cobalt-doped variants. Domain enlargement correlated with dopant concentration elevation, presumably due to the slightly larger ionic radius of cobalt cations (0.75 Å) compared to zinc cations (0.74 Å).

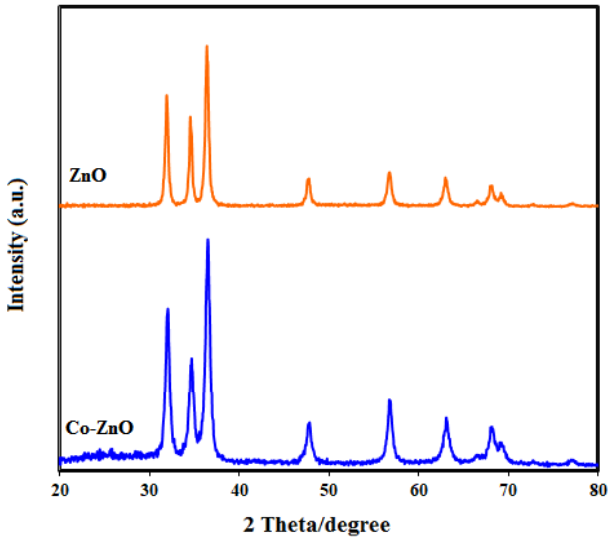

Figure 2. XRD patterns of ZnO and Co-ZnO nanoparticles.

3.2 FESEM and EDX Outcomes

Topographical configurations alongside spatial extent metrics characterizing the laboratory-fabricated specimens underwent detailed scrutiny employing FESEM imaging methodology. As displayed within the Figure 3 illustration, the representative dimensional magnitude of ZnO and Co-ZnO nanoparticles approximated 5 and 10-15 nm, respectively, with measurable enlargement of size parameters observed subsequent to transition metal integration within the host crystalline framework. The visual representation additionally corroborates that elevated dopant incorporation ratios precipitated progressive augmentation of particulate spatial dimensions. This progression corresponds with powder diffraction outcomes linking spatial enlargement to the marginally greater ionic dimensionality of cobalt cations versus zinc cations. Heteroatomic integration within the ZnO nanoscale framework was confirmed via EDX compositional analysis, as presented in Figure 4. Graphical panel four displays cobalt compositional proportions of zero percent for pristine ZnO material and 2.75 percent for cobalt-incorporated variants, further verifying minimal extraneous elemental presence in the artificially generated product.

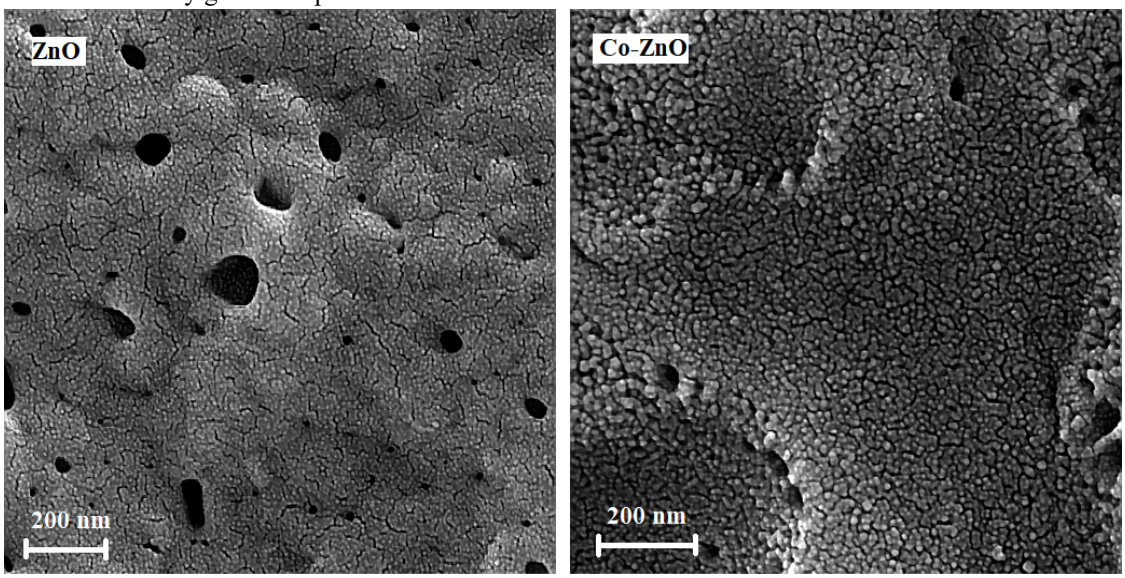

Figure 3. FESEM images of ZnO and Co-ZnO nanoparticles.

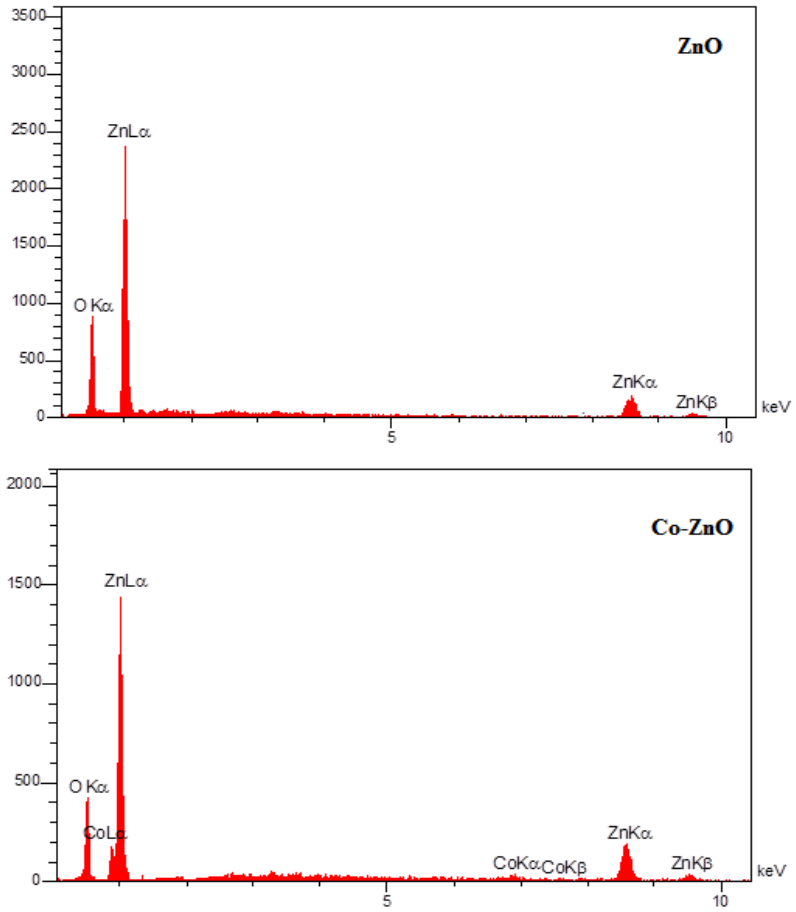

Figure 4. EDX image of ZnO and Co-ZnO nanoparticles.

3.3 Ultraviolet-visible (UV-Vis)

Figure 5 presents the UV-Vis spectral data of ZnO and Co-ZnO nanoparticles. For ZnO nanoparticles, a wavelength in the region of 340 nm is observed, which corresponds to the near-UV absorption edge and the onset of the electron transition from the valence band to the conduction band. In the Co-ZnO nanoparticles, a similar absorption profile but with a lower intensity is observed than for ZnO nanoparticles. The absorption maximum is at 340 nm and in the visible region (above 400 nm) the absorption decreases more rapidly. The decrease in absorption intensity and a slight shift of the absorption edge in the doped sample can be due to the change in the semiconductor band structure due to the substitution of cobalt ions in the ZnO lattice. Overall, both samples show strong UV absorption, which is desirable for photocatalytic and biomedical applications of these nanoparticles.

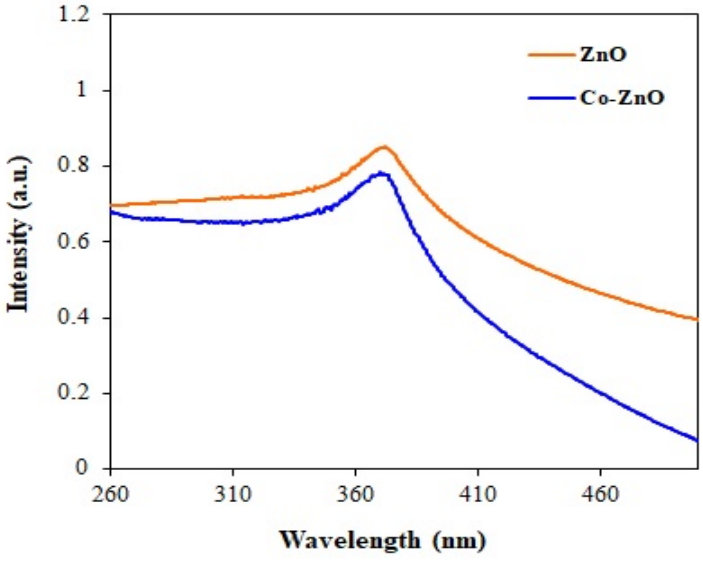

Figure 5. UV-Vis spectral of ZnO and Co-ZnO nanoparticles.

3.4 Cytotoxic Performance

Ultrafine-scale engineering has demonstrably enhanced modern oncological therapeutic protocols [50]. Elemental nanoscale assemblies, owing to their distinctive physicochemical attributes, serve as promising delivery platforms for macromolecular and small-molecule therapeutics, with ZnO constructs among the most extensively studied [51]. This study evaluated the cellular lethality of ZnO and cobalt-doped variants, laboratory-fabricated using *Prosopis farcta* phytoextract, against human cerebral grade IV glial malignancy cultures. To achieve this aim, cell populations were exposed for twenty-four hours to incrementally escalating dosage tiers (1 to 1000 µg/mL) of the ultrafine assemblies, with cellular lethality quantified via tetrazolium-based metabolic activity detection (Figure 6). The figure reveals that cobalt-integrated variants induced deleterious effects comparable to pristine ZnO specimens; however, higher dopant ratios precipitated progressively intensified cytotoxic effects. Dose-dependent amplification of cellular damage culminated at the maximal concentration (1000 µg/mL), thereby confirming lethal efficacy against human cerebral grade IV glial malignancy cultures. IC_{50} determined 320, 480, and 392 µg/mL for DOX, ZnO, and Co-ZnO nanoparticles, respectively. These results showed that the cytotoxic ability of Co-ZnO nanoparticles can compare to DOX as positive control.

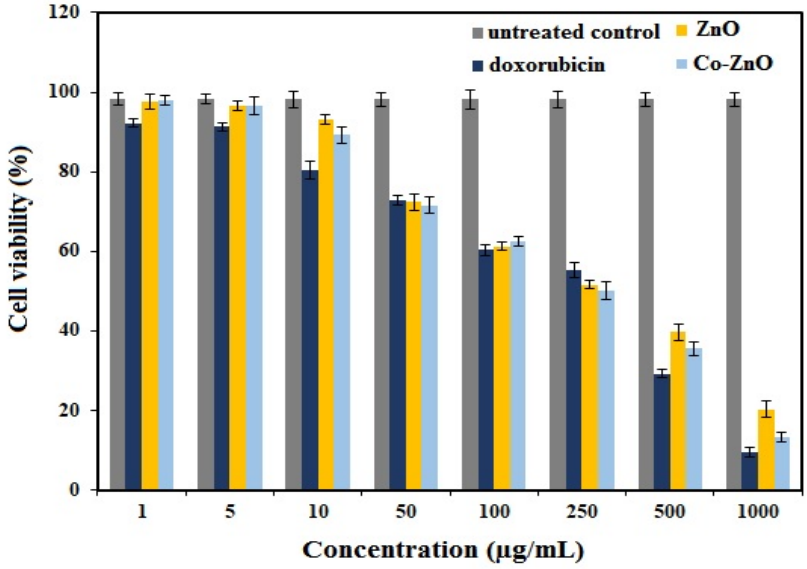

Figure 6. Cell viability of ZnO and Co-ZnO nanoparticles on U87 cell line after 24 h incubation. Experiments were conducted at 25 °C with three biological replicates (n=3).

Extensive literature documents the pronounced biological effects of phytoextract-fabricated ZnO nanoscale entities on neoplastic cells. This study examined the tumoricidal potential of ZnO particulates generated via exothermic solution-phase redox synthesis using pomegranate and tamarind organic derivatives as combustible agents. Significantly, plant-mediated variants exhibited superior cellular metabolic persistence at a maximal dosage (100 µg/mL) relative to industrially produced counterparts, which achieved only 66% viability under identical conditions [52-55].

4. Conclusion

The plant extract of *Prosopis fracta* proved to be an appropriate choice for carrying out the triumphant synthesis of ZnO and Co-ZnO nanoparticles. The physicochemical properties of this material were assessed and characterized using the results of laboratory testing equipment and analytical procedures, which confirmed the production of consistent, roughly spherical nanoparticles synthesized at the nanoscale. Progressive augmentation of the longitudinal and transverse dimensions of rod-shaped nanoscale entities was observed upon increasing cobalt dopant concentration within the ZnO crystalline framework. In following, WST-1 examination provided data on the toxic impacts of nanorods towards U87 cell line, indicating the superior inhibitory impact of doped nanoparticles than ZnO nanoparticles. It is particularly noteworthy that the cytotoxic activity of ZnO nanoparticles was increased through increasing the proportion of cobalt doped into the nanorod structure. Based on the accumulated evidence, one can confidently assert the suitability of these synthesized nanorods for applications in biological and cancer therapeutic contexts. Furthermore, these findings support their potential as a powerful and cost-effective option for the eradication of environmental pollutants.

Conflict of Interest

The authors affirm that there are no conflicts of interest.

Data Availability Statement

The documentary materials underpinning this study's findings remain accessible via the lead investigator upon reasonable request.

Generative AI Statement

The authors disclose that generative AI was just used for correct spelling errors and format references in this manuscript.

References

[1] Vijayakumar S, Vaseeharan B, Malaikozhundan B, Shobiya M. *Laurus nobilis* leaf extract mediated green synthesis of ZnO nanoparticles: Characterization and biomedical applications. Biomedicine & Pharmacotherapy. 2016, 84, 1213-1222. DOI: 10.1016/j.biopha.2016.10.038

[2] Rehman H, Ali W, Zaman Khan N, Aasim M, Khan T, Ali Khan A. *Delphinium uncinatum* mediated biosynthesis of zinc oxide nanoparticles and *in-vitro* evaluation of their antioxidant, cytotoxic, antimicrobial, anti-diabetic, anti-inflammatory, and anti-aging activities. Saudi Journal of Biological Sciences. 2023, 30(1), 103485. DOI: 10.1016/j.sjbs.2022.103485

[3] Condello M, De Berardis B, Ammendolia MG, Barone F, Condello G, Degan P, et al. ZnO nanoparticle tracking from uptake to genotoxic damage in human colon carcinoma cells. Toxicology *In Vitro*. 2016, 35, 169-179. DOI: 10.1016/j.tiv.2016.06.005

[4] Al-Hamadani NHM, Pouresmaeil V, Sharbatiyan M, Tabrizi MH. Investigation into the anticancer activity of biosynthesized zinc oxide nanoparticles incorporating 6-gingerols. Cellular and Molecular Biomedical Reports. 2025, 5(3), 168-186. DOI: 10.55705/cmbr.2025.495731.1296

[5] Li Y, Li F, Zhang L, Zhang C, Peng H, Lan F, et al. Zinc oxide nanoparticles induce mitochondrial biogenesis impairment and cardiac dysfunction in human iPSC-derived cardiomyocytes. International Journal of Nanomedicine. 2020, 15, 2669-2683. DOI: 10.2147/IJN.S249912.

[6] Dash UC, Bhol NK, Swain SK, Samal RR, Nayak PK, Raina V, et al. Oxidative stress and inflammation in the pathogenesis of neurological disorders: Mechanisms and implications. Acta Pharmaceutica Sinica B. 2025, 15(1), 15-34. DOI: 10.1016/j.apsb.2024.10.004

[7] Harshita Sharma, Pawan K. Mishra, Sushama Talegaonkar, Bhuvaneshwar Vaidya. Metal nanoparticles: A theranostic nanotool against cancer. Drug Discovery Today. 2015, 20(9), 1143-1151. DOI: 10.1016/j.drudis.2015.05.009

[8] Sharma H, Kumar K, Choudhary C, Mishra PK, Vaidya B. Development and characterization of metal oxide nanoparticles for the delivery of anticancer drug. Artificial Cells, Nanomedicine, and Biotechnology. 2016, 44(2), 672-679. DOI: 10.3109/21691401.2014.978980

[9] Wang L, Guo D, Wang Z, Yin X, Wei H, Hu W, et al. Zinc oxide nanoparticles induce human tenon fibroblast apoptosis through reactive oxygen species and caspase signaling pathway. Archives of Biochemistry and Biophysics. 2020, 683, 108324. DOI: 10.1016/j.abb.2020.108324

[10] Su L, Li H, Wang J, Wu J, Wan J, He YF, et al. Zinc oxide nanoparticles cause hepatotoxicity in rare minnow (*Gobiocypris rarus*) via ROS-mediated oxidative stress and apoptosis activation and inhibition of lipid peroxidation. Aquaculture Reports. 2024, 38(5), 102317. DOI: 10.1016/j.aqrep.2024.102317

[11] Alarifi S, Ali D, Alkahtani S, Verma A, Ahamed M, Ahmed M, et al. Induction of oxidative stress, DNA damage, and apoptosis in a malignant human skin melanoma cell line after exposure to zinc oxide nanoparticles. International Journal of Nanomedicine. 2013, 8, 983-993. DOI: 10.2147/IJN.S42028

[12] Merighi A, Lossi L. Endoplasmic reticulum stress signaling and neuronal cell death. International Journal of Molecular Sciences. 2022, 23(23), 15186. DOI: 10.3390/ijms232315186

[13] Kosmulski M. The pH dependent surface charging and points of zero charge. X. Update. Advances in Colloid and Interface Science. 2023, 319, 102973. DOI: 10.1016/j.cis.2023.102973

[14] Arulkumar E, Thanikaikarasan S, Rajkumar S, Wondimu W. Influence of solution pH dependency on structure, optical with photoelectrochemical characteristics of SILAR deposited copper oxide thin films. Heliyon. 2024, 10(13), e33579. DOI: 10.1016/j.heliyon.2024.e33579

[15] Pajic-Lijakovic I, Milivojevic M. Surface activity of cancer cells: The fusion of two cell aggregates. Biocell. 2022, 47(1), 1-18. DOI: 10.48550/arXiv.2109.09424

[16] Vallabhapurapu SD, Blanco V, Sulzmaier L, Dunleavey J, Singh S, Chu ZT, et al. Variation in human cancer cell external phosphatidylserine is regulated by flippase activity and intracellular calcium. Oncotarget. 2015, 6, 34375-34388. DOI: 10.18632/oncotarget.6045

[17] Aksoy B, Atakan N, Aksoy HM, Tezel GG, Renda N, Ozkara HA, et al. Effectiveness of topical zinc oxide application on hypertrophic scar development in rabbits. Burns. 2010, 36(7), 1027-1035. DOI: 10.1016/j.burns.2010.01.020

[18] Chakraborti S, Chakraborty S, Saha S, Manna A, Banerjee S, Adhikary A, et al. PEG-functionalized zinc oxide nanoparticles induce apoptosis in breast cancer cells through reactive oxygen species-dependent impairment of DNA damage repair enzyme NEIL2. Free Radical Biology and Medicine. 2017, 103, 35-47. DOI: 10.1016/j.freeradbiomed.2016.11.048

[19] Namvar F, Azizi S, Rahman HS, Mohamad R, Rasedee A, Soltani M, et al. Green synthesis, characterization, and anticancer activity of hyaluronan/zinc oxide nanocomposite. OncoTargets and Therapy. 2016, 9, 4549-4559. DOI: 10.2147/OTT.S95962

[20] Kc B, Paudel SN, Rayamajhi S, Karna D, Adhikari S, Shrestha BG, et al. Enhanced preferential cytotoxicity through surface modification: synthesis, characterization and comparative *in vitro* evaluation of TritonX-100 modified and unmodified zinc

oxide nanoparticles in human breast cancer cell (MDA-MB-231). Chemistry Central Journal. 2016, 10, 16. DOI: 10.1186/s13065-016-0162-3
[21] Mohamed SY, Elshoky HA, El-Sayed NM, Fahmy HM, Ali MA. Ameliorative effect of zinc oxide-chitosan conjugates on the anticancer activity of cisplatin: Approach for breast cancer treatment. International Journal of Biological Macromolecules. 2024, 257(Pt 1), 128597. DOI: 10.1016/j.ijbiomac.2023.128597
[22] Chandrasekaran M, Pandurangan M. *In vitro s*elective anti-proliferative effect of zinc oxide nanoparticles against co-cultured C2C12 myoblastoma cancer and 3T3-L1 normal cells. Biological Trace Element Research. 2016, 172, 148-154. DOI: 10.1007/s12011-015-0562-6
[23] Quispe Cohaila AB, Fora Quispe GL, Cáceda Quiroz CJ, Mamani Anccasi R, Mejía García TA, Tamayo Calderón RM, et al. Biogenic ZnO nanoparticles synthesized by B. licheniformis: A selective cytotoxicity against NG-108 glioblastoma cells. Nanomaterials. 2025, 15(17), 1338. DOI: 10.3390/nano15171338
[24] Sukhodub L, Kumeda M, Sukhodub L, Vovchenko L, Prokopiuk V, Petrenko O, et al. Effect of zinc oxide micro- and nanoparticles on cytotoxicity, antimicrobial activity and mechanical properties of apatite-polymer osteoplastic material. Journal of the Mechanical Behavior of Biomedical Materials. 2024, 150, 106289. DOI: 10.1016/j.jmbbm.2023.106289
[25] Tseriotis VS, Ampazis D, Karachrysafi S, Papamitsou T, Petrakis G, Kouvelas D, et al. ZnO-based nanoparticles for targeted cancer chemotherapy and the role of tumor microenvironment: A systematic review. International Journal of Molecular Sciences. 2025, 26(17), 8417. DOI: 10.3390/ijms26178417
[26] Han Z, Wang XH, Heng CL, Han QS, Cai SF, Li JY, et al. Synergistically enhanced photocatalytic and chemotherapeutic effects of aptamer-functionalized ZnO nanoparticles towards cancer cells. Physical Chemistry Chemical Physics. 2015, 17, 21576-21582. DOI: 10.1039/c5cp02139a
[27] Ahmadi M, Ritter CA, von Woedtke T, Bekeschus S, Wende K. Package delivered: Folate receptor-mediated transporters in cancer therapy and diagnosis. Chemical Science. 2024, 15, 1966-2006. DOI: 10.1039/d3sc05539f
[28] Vimala K, Shanthi K, Sundarraj S, Kannan S. Synergistic effect of chemo-photothermal for breast cancer therapy using folic acid (FA) modified zinc oxide nanosheet. Journal of Colloid and Interface Science. 2017, 488, 92-108. DOI: 10.1016/j.jcis.2016.10.067
[29] Davis ME. Glioblastoma: Overview of disease and treatment. Clinical Journal of Oncology Nursing. 2016, 20(5 Suppl), S2-S8. DOI: 10.1188/16.CJON.S1.2-8
[30] Akter F, Simon B, de Boer NL, Redjal N, Wakimoto H, Shah K. Pre-clinical tumor models of primary brain tumors: Challenges and opportunities. Biochimica et Biophysica Acta - Reviews on Cancer. 2021, 1875(1), 188458. DOI: 10.1016/j.bbcan.2020.188458.
[31] Alifieris C, Trafalis DT. Glioblastoma multiforme: Pathogenesis and treatment. Pharmacology & Therapeutics. 2015, 152, 63-82. DOI: 10.1016/j.pharmthera.2015.05.005
[32] Mukhtar M, Bilal M, Rahdar A, Barani M, Arshad R, Behl T, et al. Nanomaterials for diagnosis and treatment of brain cancer: Recent updates. Chemosensors. 2020, 8(4), 117. DOI: 10.3390/chemosensors8040117
[33] Mohamed NA, Marei I, Crovella S, Abou-Saleh H. Recent developments in nanomaterials-based drug delivery and upgrading treatment of cardiovascular diseases. International Journal of Molecular Sciences. 2022, 23(3), 1404. DOI: 10.3390/ijms23031404
[34] Hamidian K, Sarani M, Sheikhi E, Khatami M. Cytotoxicity evaluation of green synthesized ZnO and Ag-doped ZnO nanoparticles on brain glioblastoma cells. Journal of Molecular Structure. 2022, 1251(1), 131962. DOI: 10.1016/j.molstruc.2021.131962
[35] Harish V, Tewari D, Gaur M, Yadav AB, Swaroop S, Bechelany M, et al. Review on nanoparticles and nanostructured materials: Bioimaging, biosensing, drug delivery, tissue engineering, antimicrobial, and agro-food applications. Nanomaterials. 2022, 12(3), 457. DOI: 10.3390/nano12030457
[36] Darroudi M, Hakimi M, Sarani M, Kazemi Oskuee R, Khorsand Zak A, Gholami L, et al. Facile synthesis, characterization, and evaluation of neurotoxicity effect of cerium oxide nanoparticles. Ceramics International. 2013, 39(6), 6917-6921. DOI: 10.1016/j.ceramint.2013.02.026
[37] Hoseini SJ, Darroudi M, Kazemi Oskuee R, Gholami L, Khorsand Zak A. Honey-based synthesis of ZnO nanopowders and their cytotoxicity effects. Advanced Powder Technology. 2015, 26(3), 991-996. DOI: 10.1016/j.apt.2015.04.003
[38] Abdul Salam H, Sivaraj R, Venckatesh R. Green synthesis and characterization of zinc oxide nanoparticles from *Ocimum basilicum* L. var. *purpurascens* Benth-Lamiaceae leaf extract. Materials Letters. 2014, 131, 16-18. DOI:10.1016/j.matlet.2014.05.033
[39] Fu L, Fu Z. Plectranthus amboinicus leaf extract-assisted biosynthesis of ZnO nanoparticles and their photocatalytic activity. Ceramics International. 2015, 41(2), 2492-2496. DOI: 10.1016/j.ceramint.2014.10.069
[40] Nethravathi PC, Shruthi GS, Suresh D, Udayabhanu, Nagabhushana H, Sharma S. *Garcinia xanthochymus* mediated green synthesis of ZnO nanoparticles: Photoluminescence, photocatalytic and antioxidant activity studies. Ceramics International. 2015, 41(7), 8680-8687. DOI: 10.1016/j.ceramint.2015.03.084
[41] Jayaseelan C, Rahuman AA, Kirthi AV, Marimuthu S, Santhoshkumar T, Bagavan A, et al. Novel microbial route to synthesize ZnO nanoparticles using *Aeromonas hydrophila* and their activity against pathogenic bacteria and fungi. Spectrochimica Acta Part A: Molecular and Biomolecular Spectroscopy. 2012, 90, 78-84. DOI: 10.1016/j.saa.2012.01.006
[42] Mohammadi Dargah M, Pedram P, Cabrera-Barjas G, Delattre C, Nesic A, Santagata G, et al. Biomimetic synthesis of nanoparticles: A comprehensive review on green synthesis of nanoparticles with a focus on *Prosopis farcta* plant extracts and biomedical applications. Advances in Colloid and Interface Science. 2024, 332, 103277. DOI: 10.1016/j.cis.2024.103277
[43] Kundu D, Hazra C, Chatterjee A, Chaudhari A, Mishra S. Extracellular biosynthesis of zinc oxide nanoparticles using *Rhodococcus pyridinivorans* NT2: Multifunctional textile finishing, biosafety evaluation and *in vitro* drug delivery in colon carcinoma. Journal of Photochemistry and Photobiology B: Biology. 2014, 140, 194-204. DOI: 10.1016/j.jphotobiol.2014.08.001
[44] Azizi S, Ahmad MB, Namvar F, Mohamad R. Green biosynthesis and characterization of zinc oxide nanoparticles using brown marine macroalga *Sargassum muticum* aqueous extract. Materials Letters. 2014, 116, 275-277. DOI: 10.1016/j.matlet.2013.11.038

[45] Zamiri R, Parvizi R, Zakaria A, Sadrolhosseini AR, Zamiri G, Darroudi M, et al. Investigation on nonlinear-optical properties of palm oil/silver nanoparticles. Journal of the European Optical Society - Rapid Publications. 2012, 7, 12020. DOI: 10.2971/jeos.2012.12020
[46] Rosi NL, Mirkin CA. Nanostructures in biodiagnostics. Chemical Reviews. 2005, 105(4), 1547-1562. DOI: 10.1021/cr030067f
[47] Tania IS, Ali M. Coating of ZnO nanoparticle on cotton fabric to create a functional textile with enhanced mechanical properties. Polymers. 2021, 13(16), 2701. DOI: 10.3390/polym13162701
[48] Sangeetha G, Rajeshwari S, Venckatesh R. Green synthesis of zinc oxide nanoparticles by *Aloe barbadensis miller* leaf extract: Structure and optical properties. Materials Research Bulletin. 2011, 46(12), 2560-2566. DOI: 10.1016/j.materresbull.2011.07.046
[49] Massima Mouele ES, Tijani JO, Fatoba OO, Petrik LF. Degradation of organic pollutants and microorganisms from wastewater using different dielectric barrier discharge configurations - a critical review. Environmental Science and Pollution Research. 2015, 22(23), 18345-18362. DOI: 10.1007/s11356-015-5386-6
[50] Jeevanandam J, Barhoum A, Chan YS, Dufresne A, Danquah MK. Review on nanoparticles and nanostructured materials: History, sources, toxicity and regulations. Beilstein Journal of Nanotechnology. 2018, 9, 1050-1074. DOI: 10.3762/bjnano.9.98
[51] Jiang J, Pi J, Cai J. The advancing of zinc oxide nanoparticles for biomedical applications. Bioinorganic Chemistry and Applications. 2018, 2018(3), 1-18. DOI: 10.1155/2018/1062562
[52] Rama Narsimha Reddy A, Srividya L. Evaluation of *in vitro* cytotoxicity of zinc oxide (ZnO) nanoparticles using human cell lines. Journal of Toxicology and Risk Assessment. 2018, 4(1), 009. DOI: 10.23937/2572-4061.1510009
[53] Miri A, Sarani M. Biosynthesis and cytotoxic study of synthesized zinc oxide nanoparticles using *Salvadora persica*. BioNanoScience. 2019, 9, 164-171. DOI: 10.1007/s12668-018-0579-3
[54] Nemati S, Hosseini HA, Hashemzadeh A, Mohajeri M, Sabouri Z, Darroudi M, et al. Cytotoxicity and photocatalytic applications of biosynthesized ZnO nanoparticles by *Rheum turketanicum* rhizome extract. Materials Research Express. 2019, 6(12), 125016. DOI: 10.1088/2053-1591/ab46fb
[55] Akhtar MJ, Alhadlaq HA, Alshamsan A, Majeed Khan MA, Ahamed M. Aluminum doping tunes band gap energy level as well as oxidative stress-mediated cytotoxicity of ZnO nanoparticles in MCF-7 cells. Scientific Reports. 2015, 5, 13876. DOI: 10.1038/srep13876